Vortex dynamics and frustration in two-dimensional triangular chromium lattices

M. Hemmida,[1] H.-A. Krug von Nidda,[1] N. Büttgen,[1] A. Loidl,[1] L. K. Alexander,[2] R. Nath,[2,3] A. V. Mahajan,[2] R. F. Berger,[4] R. J. Cava,[4] Yogesh Singh,[3] and D. C. Johnston[3]

[1]*Experimental Physics V, Center for Electronic Correlations and Magnetism, University of Augsburg, 86135 Augsburg, Germany*

[2]*Department of Physics, Indian Institute of Technology, Mumbai 400076, India*

[3]*Ames Laboratory and Department of Physics and Astronomy, Iowa State University, Ames, Iowa 50011, USA*

[4]*Department of Chemistry, Princeton University, Princeton, New Jersey 08544, USA*

(Received 25 May 2009; revised manuscript received 23 July 2009; published 12 August 2009)

The spin dynamics of the two-dimensional (2D) triangular lattice antiferromagnets $HCrO_2$, $LiCrO_2$, and $NaCrO_2$ is investigated by electron spin resonance. In these oxides, on approaching the Néel temperature T_N from above, the divergence of the temperature dependent linewidth is well described in terms of a Berezinskii-Kosterlitz-Thouless scenario due to magnetic vortex-antivortex pairing. A refined analysis suggests analogies to the melting scenario of a 2D triangular lattice described by Nelson, Halperin, and Young.

DOI: 10.1103/PhysRevB.80.054406 PACS number(s): 75.50.Ee, 75.40.Gb, 76.30.Fc

I. INTRODUCTION

Triangular lattice antiferromagnets, from the viewpoint of spin frustration and emerging exotic ground states, are very interesting.[1,2] They are widely studied in a search for unconventional magnetic order. One of these exotic ground states is the spin-liquid state proposed for the $S=1/2$ triangular Heisenberg antiferromagnet by P. W. Anderson in 1973.[3] He suggested, due to geometrical frustration, that the ground state—the so-called resonant valence-bond state—may be described by an assembly of randomly distributed movable open singlet pairs on a two-dimensional Heisenberg triangular lattice. The discovery of superconductivity[4] in $Na_xCoO_2 \cdot yH_2O$ has recently motivated further research in related triangular layered alkali transition-metal oxides.

We focus here on the magnetic behavior of $HCrO_2$, $LiCrO_2$, and $NaCrO_2$ which crystallize in the ordered rock-salt structure (space group $R\bar{3}m$). The corresponding in-plane antiferromagnetic exchange constants J (Refs. 5 and 6) and the antiferromagnetic ordering temperatures T_N (Refs. 5 and 7–9) are listed in the upper part of Table I. In $NaCrO_2$ muon-spin rotation (μSR) and nuclear magnetic resonance (NMR) additionally probe strong fluctuations below T_N with a broad peak of the relaxation rate $1/T_1$ around $T=25$ K.[9] Previous electron spin resonance (ESR) experiments revealed a divergent broadening of the single resonance line on approaching T_N which was ascribed to critical fluctuations due to frustration[10–12] or to the influence of magnetic vortices[5] in all three compounds. In the present work, we derive information on the nature of the vortex dynamics in 2D triangular lattice antiferromagnets from the analysis of the ESR line broadening in $HCrO_2$, $LiCrO_2$, and $NaCrO_2$. Our results demonstrate the relevance of vortices for the spin relaxation in such magnetically frustrated systems.

II. THEORETICAL BACKGROUND

An important aspect of two-dimensional (2D) systems is the topological defect. As early as 1971, Berezinskii[13] suggested vortices as topological defects. Based on these ideas, Kosterlitz and Thouless[14] formulated a theory of a vortex-mediated phase transition in the two-dimensional XY model into a so called topological phase. This ground state is different from both the long-range order of the 2D Ising model[15] and the disorder down to zero temperature of the 2D Heisenberg model.[16] Below a certain critical temperature, the Kosterlitz-Thouless temperature T_{KT}, vortices, and antivortices are bound in vortex-antivortex pairs. Detailed theoretical investigations revealed that the existence of magnetic vortices and the Kosterlitz-Thouless transition is not confined to the pure XY model, but even a weak planar anisotropy is enough to provide for vortex excitations in a 2D magnet.[17] More importantly, the 2D triangular Heisenberg antiferromagnet has been discussed to show a Kosterlitz-Thouless-like transition, in analogy to the 2D XY ferromagnet[18] with another type of vortices. These so-called Z_2 vortices are characterized by a two-valued topological quantum number only, instead of an infinite variety as in the case of Berezinskii-Kosterlitz-Thouless (BKT) vortices. These results encourage research in order to search for vortices in the triangular chromium oxides, although being of dominant Heisenberg character, as confirmed by susceptibility and antiferromagnetic resonance measurements in single crystals.[11,19]

It is important to note that in real 2D magnets a residual interaction $J' \ll J$ between neighboring magnetic layers always exists. This interlayer interaction, together with the anisotropy of the intralayer interaction, can give rise to formation of 3D long-range order. It was shown that for the XY model with interplanar coupling the ordering temperature T_N is expected to be somewhat larger than T_{KT} and, consequently, the BKT transition is masked by 3D magnetic order.[20] However, the tendency to undergo a BKT transition can be anticipated from the vortex dynamics in the paramagnetic phase. Experimental indications of a BKT phase transition in a 2D magnet were found in the honeycomb layer system $BaNi_2P_2O_8$ using NMR (Refs. 21) and recently by ESR in the isostructural compound $BaNi_2V_2O_8$.[22] Inelastic neutron scattering (INS) successfully detected the characteristic divergence of the correlation length from the structure factor in $MnPS_3$,[23] which also crystallizes in honeycomb structure. The anisotropic field dependence of the Curie temperature T_C detected with ferromagnetic resonance experiments in the square lattice 2D ferromagnets K_2CuF_4 and

$(CH_3NH_3)_2CuCl_4$ was interpreted in terms of a BKT scenario.[24] Recent high-field ESR investigations suggest the occurrence of the Z_2 vortices in $NiGa_2S_4$.[25]

[A]To understand the influence of the vortices on experimental observables one has to primarily consider the static part of the two spin-correlation function[26] which reads for $T > T_{KT}$

$$\langle S_x(0)S_x(r)\rangle \approx \frac{\exp[-r/\xi(T))]}{\sqrt{r}} \quad (1)$$

wherein r denotes the distance between two spins S under consideration. In the XY model the correlation length $\xi(T)$ reveals an exponential divergence at T_{KT} following

$$\xi(T) = \xi_0 \exp(b/\tau^{\nu}) \quad (2)$$

with $\tau=(T/T_{KT}-1)$, $\nu=0.5$, and $b\approx 1.5$;[27] ξ_0 is of the order of the lattice constant. The correlation length $\xi(T)$ is related to the density of free vortices $n_v \simeq (2\xi)^{-2}$ and, thus, can be interpreted as the average half distance between two free vortices.[26] In the triangular lattice Heisenberg antiferromagnet Monte Carlo simulations indicated that the spin-correlation function decays exponentially as in the 2D XY model above the transition temperature,[18] but the temperature dependence of the correlation length has not been calculated, yet.

INS and magnetic resonance techniques are sensitive to the dynamic structure factor $S(\mathbf{Q},\omega)$, which represents the Fourier transformation of the time and space dependent two spin-correlation function $\langle \mathbf{S}(0,0)\mathbf{S}(\mathbf{r},t)\rangle$. While INS can detect $S(\mathbf{Q},\omega)$ in the full range of frequencies ω and wave vectors $\mathbf{Q}$, NMR measures the average over $\mathbf{Q}$ at $\omega\approx 0$ via the nuclear spin-lattice relaxation rate $1/T_1$, which, in turn, can be related to the correlation length ξ.[21,28,29] In ESR the linewidth ΔH is determined by four spin-correlation functions, which in independent-mode approximation can be factorized into products of two spin-correlation functions evaluated at the wave vector of magnetic order and $\omega\approx 0$.[28] The influence of the vortex dynamics on the ESR linewidth was approximately derived by detailed calculations as $\Delta H \propto \xi^3$.[30]

III. EXPERIMENTAL RESULTS AND DISCUSSION

The ESR measurements were performed on a Bruker ELEXSYS E500-CW spectrometer at X band (9.4 GHz) frequency, equipped with a continuous He-gas flow cryostat (Oxford instruments) working in the temperature range $4.2 \leq T \leq 300$ K. $HCrO_2$ was prepared using a hydrothermal method as follows: freshly prepared CrO_2 (Ref. 31) was put in a 1 M LiOH solution in deionized water and heated to 200 °C in a teflon-lined stainless-steel autoclave. This temperature was held constant for a week and subsequently the sample was furnace cooled. Powder x-ray diffraction of the dark brown powder confirmed the proper formation of $HCrO_2$. The samples of $LiCrO_2$ and $NaCrO_2$ investigated here are taken from the same batches as those used for the experiments described in Refs. 7 and 9, respectively. The polycrystalline samples were fixed in a quartz tube with paraffin for the ESR measurements. The field derivative of the microwave-absorption signal is detected as a function of the static magnetic field due to the lock-in technique with field modulation. Resonance absorption will occur, if the incident microwave energy matches the energy of magnetic dipolar transitions between the electronic Zeeman levels.

Typical ESR spectra of $HCrO_2$, $LiCrO_2$, and $NaCrO_2$ are shown in Fig. 1. All compounds reveal a single exchange-narrowed resonance line, which is perfectly described by a Lorentzian curve. The temperature dependence of the corresponding fit parameters, i.e., intensity, resonance field, and linewidth, is illustrated in Fig. 2. The intensities have been normalized by the molar masses of the samples and represent the spin susceptibilities of the three compounds in the correct relative magnitudes. $HCrO_2$ and $NaCrO_2$ clearly reveal the characteristic maximum of two-dimensional antiferromagnets, which scales with the exchange constant J, while in

TABLE I. Exchange constant J,[5,6] Néel temperature T_N,[5,7,8] and fit parameters for the temperature dependence of the ESR linewidth corresponding to critical behavior $\Delta H = C/(T/T_N-1)^p$, BKT model $\Delta H = \Delta H_\infty \exp(3b/\tau^{0.5})$ with $\tau = T/T_{KT}-1$, and KTHNY model $\Delta H = \Delta H_\infty \exp(3b/\tau^{0.37})$ with $\tau = T/T_m - 1$. In the last part of the table, the exponent ν was given free. The quality of the fit is characterized by the coefficient of determination $R^2 = 1-\Sigma_i(y_i - f_i)^2/\Sigma_i(y_i-\bar{y})^2$, where y_i, f_i, and $\bar{y}$ denote the data, the corresponding fit values, and the total average of the data, respectively.

	$HCrO_2$	$LiCrO_2$	$NaCrO_2$
J/k_B(K)	−12	−39	−20
T_N(K)	20	62	41
Critical behavior			
C(Oe)	1822(81)	318(2)	1147(15)
p	0.78(1)	0.69(1)	0.85(1)
T_N(K)	23.3(5)	65.2(1)	36.0(2)
R^2	0.99771	0.99848	0.99895
BKT model			
ΔH_∞(Oe)	94(3)	75(1)	77(1)
b	4.1(5)	0.52(1)	1.49(2)
T_{KT}(K)	2.6(6)	56.8(1)	19.2(2)
R^2	0.99863	0.99981	0.99974
KTHNY model			
ΔH_∞(Oe)	55(2)	46.5(3)	43.5(5)
b	2.0(1)	0.67(1)	1.41(1)
T_m(K)	8.4(6)	58.9(1)	23.9(1)
R^2	0.99861	0.99994	0.99977
BKT model with free ν			
ΔH_∞(Oe)	84(22)	44(2)	48(7)
b	3.0(1.5)	0.69(1)	1.40(1)
T_{KT}(K)	4(3)	59.1(1)	23(1)
ν	0.47(8)	0.36(1)	0.39(3)
R^2	0.99864	0.99995	0.99977

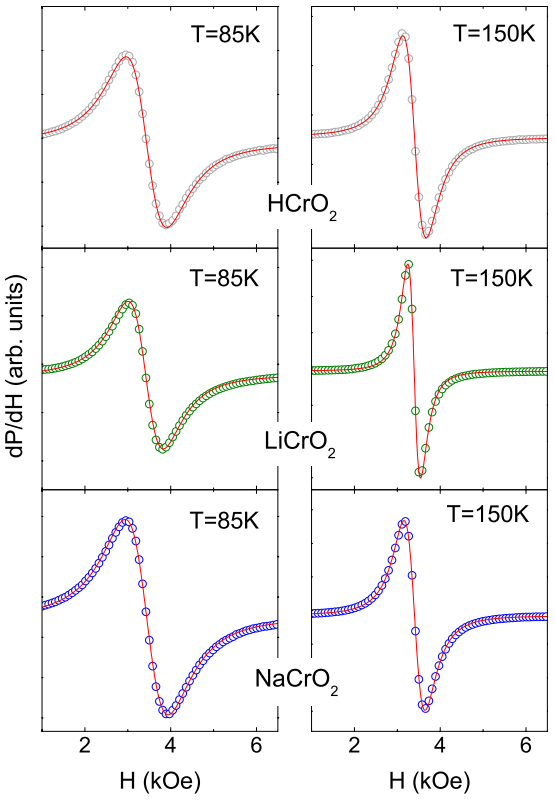

FIG. 1. (Color online) ESR spectra of $HCrO_2$, $LiCrO_2$, and $NaCrO_2$ in X-band for selected temperatures in the paramagnetic regime. The solid line indicates the fit with the field derivative of a Lorentz line.

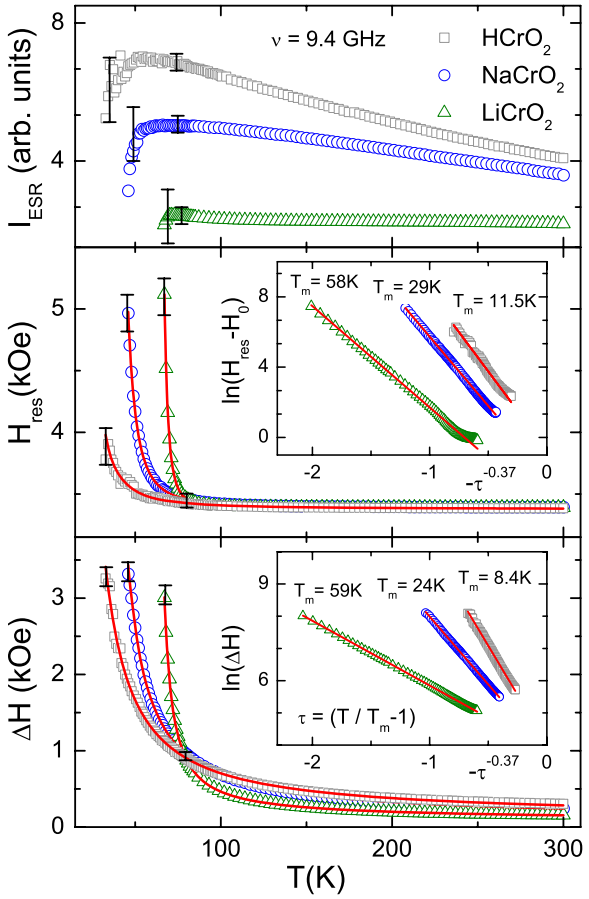

FIG. 2. (Color online) Temperature dependence of the intensity, resonance field, and linewidth in $HCrO_2$, $LiCrO_2$, and $NaCrO_2$. Typical error bars corresponding to 5% uncertainty of the linewidth are shown. Their magnitude becomes smaller than the symbol size for $T>100$ K. The fit in terms of KTHNY scenario is described in the text. Insets: Logarithmic plots of the linewidth in $HCrO_2$, $LiCrO_2$, and $NaCrO_2$ in the full-accessible temperature range; middle frame: $\ln(H_{res}-H_0)$ vs $-\tau^{-0.37}$, where H_0 denotes the resonance field without interaction, lower frame: $\ln(\Delta H)$ vs $-\tau^{-0.37}$.

$LiCrO_2$ the susceptibility is rather flat due to the higher exchange coupling. At elevated temperatures the resonance fields of all three compounds correspond to a g value of about $g=2$ indicating the quenched orbital moment of the half-filled t_{2g} state in Cr^{3+} with pure spin $S=3/2$. The linewidth at room temperature amounts to about 300 Oe, 150 Oe, and 280 Oe for the H, Li and Na system, respectively. The spectra broaden rapidly, shifting to higher resonance fields and becoming undetectable on approaching T_N.

To characterize this divergence, the temperature dependence of the linewidth was analyzed in terms of critical behavior and the BKT model, as in Ref. 22, but without any residual constant or linear contributions. Both models yield a satisfactory fitting of the linewidth data in the whole temperature range and the corresponding results are summarized in Table I.[32] In regard to the critical behavior, the parameter T_N approximates the literature values for all three compounds within an error bar of 5–14%. The critical exponent attains values of $p\approx 0.69-0.85$, in satisfactory agreement with Refs. 5 and 12. This value is rather small and theoretically unexpected for two-dimensional magnets[28] where such low exponents usually appear only near T_N due to 3D antiferromagnetic fluctuations.

The BKT model is more favorable in all three compounds considering the coefficient of determination R^2. Contrary to previous applications of this model on ESR or NMR data,[21,22,30] where either only a narrow temperature regime near T_N was evaluated or additional relaxation contributions had to be added in order to fit a broader temperature regime, we now achieve an excellent description of the whole temperature range $T_N\leq T\leq 300$ K by the BKT scenario only, without adding any residual linewidth contribution. This establishes the dominant role of magnetic vortices for the spin relaxation in these systems.

In $LiCrO_2$ the ratio $T_{KT}\approx 0.9T_N$ is typical for a BKT transition.[21] The small value of $b=0.52$, however, is not in contradiction with theory, because this depends on the details of the underlying model and values lower than 1.5 were achieved in calculations as well.[26,33] These observations are supported by recent NMR experiments in $LiCrO_2$, which obtained a BKT transition at 55 K from the temperature dependence of the ^{7}Li nuclear spin-lattice relaxation rate.[7] For $NaCrO_2$ the parameter $b=1.49$ fairly agrees with the value 1.5 derived from early calculations,[27] whereas the ratio $T_{KT}\approx 0.5T_N$ is rather small. For $HCrO_2$ the ratio $T_{KT}\approx 0.13T_N$ is even smaller and the value of $b\approx 4.1$ unexpectedly large.

For further analysis of the data we recall the broad peak around 25 K found in the μSR data for $NaCrO_2$, which in-

dicates strong magnetic fluctuations even below T_N and was interpreted as a gradual freezing into the ground state.[9] Such a scenario is strongly reminiscent to the refined BKT model developed by Halperin and Nelson[34] and independently established by Young.[35] This Kosterlitz-Thouless-Halperin-Nelson-Young (KTHNY) model extends the original ideas of Kosterlitz and Thouless to describe the two-dimensional melting mechanism in the Coulomb gas on a triangular lattice. The resulting correlation length is similar to Eq. (2) with a modified exponent $\nu \approx 0.37$ and with an arbitrary b parameter value. T_{KT} is substituted by the melting temperature T_m in τ.

All linewidth data are very well described, using the modified correlation length of the KTHNY model, as illustrated in the lower panel of Fig. 2. The R^2 values are even improved as compared to the BKT fit for Li and $NaCrO_2$. The logarithmic plot of ΔH vs. $\tau^{-0.37}$ shown in the inset reveals a linear dependence in the whole temperature range under consideration. For the record, using the exponent ν as free fourth fit parameter yields $\nu=0.36(1)$, 0.39(3), and 0.47(8) for Li, Na, and $HCrO_2$, respectively. In this way Li and $NaCrO_2$ are preferably described in terms of the KTHNY model. The other fit-parameter values such as ΔH_∞, b, and T_{KT} as well as R^2 are also comparable to those obtained in the KTHNY model (see Table I). For $HCrO_2$ the exponent ν lies close to 0.5, but with a large error bar. The other fit parameters exhibit quite large uncertainties, as well. The R^2 value is, moreover, rather similar for BKT, KTHNY, and free ν fitting. Therefore, there is no clear preference for one of these approaches in $HCrO_2$.

The middle frame of Fig. 2 shows that the resonance fields can be simultaneously described by the melting scenario with slightly different T_m, although theoretical predictions do not exist yet. For $LiCrO_2$, T_m is close to T_N indicating only minor importance of fluctuations below T_N and in accordance with the well-defined 3D magnetic order established by neutron scattering.[8,19] Very recently, a peak was observed in the μSR relaxation at about $0.9T_N \approx 56$ K, which is very close to T_m indicating a narrowed fluctuation regime below T_N.[36] In $NaCrO_2$ the melting temperature $T_m = 24$ K is in good agreement with the μSR-relaxation peak, confirming the extended fluctuation regime. This is also supported by neutron scattering detecting long-range order within the triangular planes only, but no definite magnetic periodicity along the c direction in $NaCrO_2$, due to a high number of short-range defects.[8] Recent high-resolution neutron scattering reveals a weak incommensurate modulation along the c axis, suggesting interlayer frustration.[37] It is important to note that the 2D melting transition—from a well-ordered solid into a disordered liquid—is characterized by an intermediate liquid-crystal phase for $T_m \leq T \leq T_i$. In our opinion the above evaluation suggests that in 2D magnetic systems under consideration T_N corresponds to T_i.

IV. SUMMARY

In conclusion we have shown that the spin relaxation in the two-dimensional frustrated triangular lattice antiferromagnets $HCrO_2$, $LiCrO_2$, and $NaCrO_2$ can be fully ascribed to magnetic vortices without any residual contributions in the temperature regime $T_N \leq T \leq 300$ K. As these systems are of dominant Heisenberg character, Z_2 vortices are expected. Monte Carlo simulations showed that the spin-correlation function in the triangular lattice Heisenberg antiferromagnet decays exponentially, as in the 2D XY model above the transition temperature.[18] The temperature dependence of the correlation length has, however, not been calculated, yet. Hence, our ESR results suggest a similar temperature dependence as in the case of BKT vortices but with the modified exponent $\nu=0.37$. The applicability of the KTHNY model to two-dimensional magnets in the presence of strong geometrical frustration motivates further theoretical and experimental investigations.

ACKNOWLEDGMENTS

We are grateful to A. P. Kampf, T. Kopp, A. Krimmel, A. Skroblies, and D. V. Zakharov for fruitful discussions. This work was supported by DFG within SFB 484 (Augsburg). M.H. was partially supported by DAAD.

[1] M. F. Collins and O. A. Petrenko, Can. J. Phys. **75**, 605 (1997).
[2] H. Kawamura, J. Phys.: Condens. Matter **10**, 4707 (1998).
[3] P. W. Anderson, Mater. Res. Bull. **8**, 153 (1973).
[4] K. Takada, H. Sakurai, E. Takayama-Muromachi, F. Izumi, R. A. Dilanian, and T. Sasaki, Nature (London) **422**, 53 (2003).
[5] Y. Ajiro, H. Kikuchi, S. Sugiyama, T. Nakashima, S. Shamoto, N. Nakayama, M. Kiyama, N. Yamamoto, and Y. Oka, J. Phys. Soc. Jpn. **57**, 2268 (1988).
[6] C. Delmas, F. Menil, G. Le Flem, C. Fouassier, and P. Hagenmuller, J. Phys. Chem. Solids **39**, 55 (1978).
[7] L. K. Alexander, N. Buttgen, R. Nath, A. V. Mahajan, and A. Loidl, Phys. Rev. B **76**, 064429 (2007).
[8] J. L. Soubeyroux, D. Fruchart, C. Delmas, and G. Le Flem, J. Magn. Magn. Mater. **14**, 159 (1979).
[9] A. Olariu, P. Mendels, F. Bert, B. G. Ueland, P. Schiffer, R. F. Berger, and R. J. Cava, Phys. Rev. Lett. **97**, 167203 (2006).
[10] S. Angelov, J. Darriet, C. Delmas, and G. L. Flem, Solid State Commun. **50**, 345 (1984).
[11] P. R. Elliston, F. Habbal, N. Saleh, G. E. Watson, K. W. Blazey, and H. Rohrer, J. Phys. Chem. Solids **36**, 877 (1975).
[12] N. O. Moreno, C. Israel, P. G. Pagliuso, A. J. Garcia-Adeva, C. Rettori, J. L. Sarraoa, J. D. Thompson, and S. B. Oseroff, J. Magn. Magn. Mater. **272–276**, E1023 (2004).
[13] V. L. Berezinskii, Zh. Eksp. Teor. Fiz. **59**, 907 (1970) [Sov. Phys. JETP **32**, 493 (1971)].
[14] J. M. Kosterlitz and D. J. Thouless, J. Phys. C **6**, 1181 (1973).
[15] L. Onsager, Phys. Rev. **65**, 117 (1944).
[16] N. D. Mermin and H. Wagner, Phys. Rev. Lett. **17**, 1133 (1966).
[17] A. Cuccoli, T. Roscilde, R. Vaia, and P. Verrucchi, Phys. Rev. Lett. **90**, 167205 (2003).

[18] H. Kawamura and S. Miyashita, J. Phys. Soc. Jpn. **53**, 4138 (1984).
[19] H. Kadowaki, H. Takei, and K. Motoya, J. Phys.: Condens. Matter **7**, 6869 (1995).
[20] S. Hikami and T. Tsuneto, Prog. Theor. Phys. **63**, 387 (1980).
[21] P. Gaveau, J. P. Boucher, L. P. Regnault, and Y. Henry, J. Appl. Phys. **69**, 6228 (1991).
[22] M. Heinrich, H.-A. Krug von Nidda, A. Loidl, N. Rogado, and R. J. Cava, Phys. Rev. Lett. **91**, 137601 (2003).
[23] H. M. Rønnow, A. R. Wildes, and S. T. Bramwell, Physica B **276-278**, 676 (2000).
[24] S. O. Demokritov, M. M. Kreines, V. I. Kudinov, and S. V. Detra, Zh. Eksp. Teor. Fiz. **95**, 2211 (1989) [Sov. Phys. JETP **68**, 1277 (1989)].
[25] H. Yamaguchi, S. Kimura, M. Hagiwara, Y. Nambu, S. Nakatsuji, Y. Maeno, and K. Kindo, Phys. Rev. B **78**, 180404(R) (2008).
[26] F. G. Mertens, A. R. Bishop, G. M. Wysin, and C. Kawabata, Phys. Rev. B **39**, 591 (1989).
[27] J. M. Kosterlitz, J. Phys. C **7**, 1046 (1974).
[28] H. Benner and J. B. Boucher, in *Magnetic Properties of Layered Transition Metal Compounds*, edited by L. J. deJongh (Kluwer, Netherlands, 1990), p. 323.
[29] F. Borsa, M. Corti, T. Goto, A. Rigamonti, D. C. Johnston, and F. C. Chou, Phys. Rev. B **45**, 5756 (1992).
[30] J. Becker, Ph. D. thesis, TU Darmstadt (1996).
[31] A. Bajpai and A. K. Nigam, Appl. Phys. Lett. **87**, 222502 (2005).
[32] The classical 2D Heisenberg model did not yield a fitting of comparable quality, which is not shown here.
[33] S. W. Heinekamp and R. A. Pelcovits, Phys. Rev. B **32**, 4528 (1985).
[34] B. I. Halperin and D. R. Nelson, Phys. Rev. Lett. **41**, 121 (1978).
[35] A. P. Young, Phys. Rev. B **19**, 1855 (1979).
[36] A. Olariu, P. Mendels, F. Bert, L. K. Alexander, A. V. Mahajan, A. D. Hillier, and A. Amato, Phys. Rev. B **79**, 224401 (2009).
[37] D. Hsieh, D. Qian, R. F. Berger, R. J. Cava, J. W. Lynn, Q. Huang, and M. Z. Hasan, Physica B **403**, 1341 (2008).